IEEE Access
Multidisciplinary | Rapid Review | Open Access Journal

Received April 14, 2022, accepted May 16, 2022, date of publication May 23, 2022, date of current version May 27, 2022.

Digital Object Identifier 10.1109/ACCESS.2022.3177196

Real-Time Power Line Detection for Safe Flight of Agricultural Spraying Drones Using Embedded Systems and Deep Learning

HYUN-SIK SON[1,2], DEOK-KEUN KIM[2,3], SEUNG-HWAN YANG[2], AND YOUNG-KIU CHOI[1]

[1]Department of Electrical and Computer Engineering, Pusan National University, Geumjeong-gu, Busan 43241, Republic of Korea
[2]Smart Agricultural Machinery R&D Group, Korea Institute of Industrial Technology, Gimje-si, Jeollabuk-do 54325, Republic of Korea
[3]Interdisciplinary Program in Agricultural and Life Science, Chonnam National University, Buk-gu, Gwangju 61186, Republic of Korea

Corresponding authors: Seung-Hwan Yang (yangsh@kitech.re.kr) and Young-Kiu Choi (ykichoi@pusan.ac.kr)

This work was supported in part by the Ministry of Small and Medium Enterprises and Startups (MSS), South Korea, through the Regional Specialized Industry Development Program supervised by the Korea Institute for Advancement of Technology (KIAT) under Grant P0002732; and in part by the Korea Institute of Industrial Technology through the Development of Holonic Manufacturing System for Future Industrial Environment under Grant kitech EO-22-0001.

ABSTRACT Power line detection is necessary for the safe flight of low-flying UAVs (Unmanned Aerial Vehicles). This paper deals with the power line recognition problem for the safety of agricultural spraying drones in agricultural environments. The dataset of power lines was obtained in an agricultural environment. The training dataset was constructed by labeling powerlines with bounding boxes of 6 sizes, ranging from 0.03 to 0.15 times the image. The model used for training was the tiny-YOLOv3 model. The model was verified using the mean average precision (mAP), which was used to verify the object recognition performance. Depending on the six sizes of bounding boxes, the mAPs were evaluated to be 70.22, 94.00, 86.75, 68.87, 61.65, and 53.40, respectively. The mAP was the highest at the bounding box of 0.05 times the image size, and it was confirmed that this size is most suitable for power line detection. The real-time frames per second (FPS) results of power lines detection are on average 12.5. This paper shows that the location detection of power lines is possible in real-time using deep-learning techniques with embedded systems.

INDEX TERMS Power line detection, deep learning, agricultural spraying drone, unmanned aerial vehicle (UAV).

I. INTRODUCTION

As drone control technology advances, it is used in various fields, such as surveillance, investigation, and agriculture [1]–[3]. Recent research on drones has led to obstacle detection and collision avoidance topics. The power line is one of the most dangerous obstacles for flying drones [4]. Since power lines are difficult to recognize for drone pilots at a long distance, there is a high risk of a drone collision. Power lines are difficult to observe when at a long distance from the drone pilot. They are mainly invisible during rainy or foggy weather. Thus, wire-strike accidents have become a significant threat to the safety of drones.

Previous studies have shown several methods for power line detection. Power line detection has been conducted using several ways, such as the Hough transform using radar images of active millimeter-wave sensors [5], the Hough transform and line tracking algorithm using images from the camera [6], and matching and grouping several line segments from collinearity properties using LiDAR [7]. Recently, studies using deep learning get increased. The studies using a convolutional neural network to detect power lines showed whether the image contained power lines but could not show the location of the power lines [8]. Using the instance segmentation, the individual location of power lines could be detected [9]. The technique using instance segmentation shows good performance in detecting diverse objects. Still, a lot of time and effort for preprocessing is required due to labeling at the pixel level. Constructing the training data using the bounding box method takes less preprocessing time than the instance segment. However, it has mainly been used to recognize a single object [10]–[12]. The main contribution of this research is as follows:

1) This study proposed technology for learning and detecting power lines using the bounding box method. A power line was trained through many successive

The associate editor coordinating the review of this manuscript and approving it for publication was Shafiqul Islam.

labeling boxes. Then, the optimal power line recognition condition was found while adjusting the size of the labeling box.

2) A new method to verify the performance of continuous object detection has been proposed. The method to verify object detection performance presented in previous studies was not suitable for continuous object detection.

This study was conducted to develop a technical element for the safe flight of agricultural spraying drones. High payload and long flight time are important for agricultural spraying drones. Therefore, it is necessary to reduce weight and power consumption. It is better to use light sensors, such as CMOS cameras, than heavy sensors, such as Light Detection and Ranging (LiDAR). Also, embedded computers for using the deep learning model have to have lightweight and low power consumption. In this study, Jetson Nano was used as embedded computers for using the deep learning model, and the tiny-YOLOv3 [13]–[14] was used due to the performance constraints of embedded computers. The deep learning model for the power line detection was set in the embedded computer of the test drone. This test drone was tested in indoor and paddy fields, and it was confirmed that the power lines were normally detected.

II. RELATED WORK

A. POWER LINE DETECTION

To support cascaded Power Line Detection(PLD), a new object recognition definition with special features of power lines in joint RGB-NIR images has been proposed [4]. This new definition of object recognition combines the line edges of pixels, the area-based special material properties of NIR, and the overall coherent color of RGB. To solve the power line object detection problem, the edge line of the wire object is first detected in the combined RGB-NIR image. More precisely, it constructs a region of the wire object using its two corresponding edge candidates. Potential powerline regions are found based on the local intensity of the NIR image. Finally, the powerline object was validated according to the uniform color characteristics of the RGB image. It was detected within 2 seconds on the PC using the PLD method from images of 1024 × 650 size. The accuracy was greater than 88% using the true positive rate.

A framework using Hough Transform and Support Vector Machine (SVM) was proposed to detect power lines in millimeter-wave radar images for helicopters [5]. An appropriate function to characterize the Bragg pattern was derived so that the classifier can be used for reliable classification. An overlapping slice processing method that facilitates parallel processing was used to improve detection accuracy. An adaptive algorithm that adjusts the probability of frames containing power lines has been proposed. This algorithm is able to detect power lines even in the presence of severe noise. A millimeter-wave lidar image with a size of 2048 × 174 was used, and a processing time per frame was evaluated at approximately 0.1 seconds. The power line detection accuracy was more than 98%.

Power line detection tests were conducted in two cases: synthetic image and real image using Hough transform, random Hough transform, and line tracking algorithm [6]. The test images were taken from a smartphone camera with a resolution of 5312 × 2988. The detection accuracy was obtained as the average pixel deviation of the detected line from the best-matched ground truth line. The detection rate is the percentage of power lines detected with an accuracy of fewer than 10 pixels. Power lines with larger pixel deviations are treated as undetected. The processing time is the average time spent per image excluding user input time to the line tracer. The detection rate was 85.71%, the detection accuracy was 3.11px, and the processing time was 5.55 seconds.

The detection and extension of the power line are predicted by estimating the mathematical model [7]. The Power Line LiDAR-based Detection and Modeling (PL^2DM) is a scan-based algorithm that uses planar analysis to segment a point cloud through minimum range-based neighbor comparison and extracts a set of power line candidate points. These points are fitted to line segments that are further matched and appropriately grouped, according to their collinearity properties. The final estimated mathematical model of the power line is expressed as a horizontal straight line combined with a vertical catenary curve. The analysis is divided into two parts. One considers the vertical displacement (in the Z direction) due to the difference in elevation angles. The other relates to the horizontal displacement (in the XY plane) concerning the azimuth. The vertical mean error is 0.078 m, and the horizontal mean error is 0.12 m.

Two CNN-based power line detection methods have been proposed for use in real-time alarm systems [8]. In the first method, end-to-end classification, the CNN is modified for the target task and jointly trained. In the second method, CNN feature classification, features are extracted from the intermediate stage of the CNN and input to the classifier. The proposed method detects power lines with errors of less than 0.3%.

A Transmission Line Detection (TLD) method based on the instance segmentation framework has been proposed[9]. Using CableNet, deep multitasking neural network, it is possible not only to segment the pixels of a transmission line from the background, but also to correlate them with the cable instances that contain those pixels. Specific structures such as dilated convolutional layers and spatial convolutional layers were introduced to improve the framework of general segmentation models by considering the appearance characteristics of cables. In addition, the two output branches are superimposed with the decoder part to produce multiple feature-embedded representations of the pixel. Finally, pixel clustering is performed to achieve accurate cable instance segmentation. By training two data sets, the true positive rates were 64.77% and 85.43%.

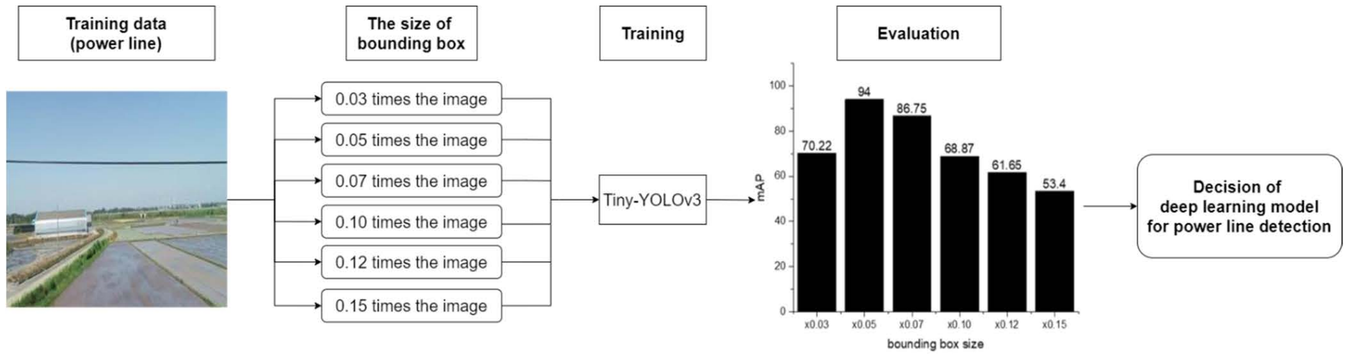

FIGURE 1. **The process to acquire a deep-learning model for power line detection.**

B. OTHER LINE DETECTION

A lane detection technology has been proposed that uses a computer vision-based algorithm to detect the road's lanes and curves, and warn the driver [15]. The technology uses multi-threshold algorithms such as the Sobel threshold and HLS threshold and uses a sliding window technique to delimit road lanes. The proposed algorithm can be implemented in real-time on a road with lanes.

A full guide system for UAVs based on image processing technology was proposed [16]. The software part consists of two algorithms. The first algorithm is crop row detection, which has been proposed and used for the identification of plant lines. The second algorithm is the line follower algorithm, which is used to move the vehicle based on the line identified by line detection. The trajectory is generated based on the identification of the planting line and the positioning parameters provided by the line follower algorithm. Then, the complete trajectory was defined at runtime using all the positioning parameters generated by the proposed algorithm. In field experiments, the algorithm achieved a 100% detection rate of crop rows for images with a resolution of 320×240 or higher. The system performance measured in the laboratory experiment was confirmed to be 31.22 FPS at the resolution of 320×240 and 1.63 FPS at the resolution of 1920×1080.

III. METHODS

The training data were labeled with bounding boxes of various sizes and trained with tiny-YOLOv3. Through evaluation metrics, an optimized bounding box was decided. Finally, a deep learning model was obtained for power line detection(Fig. 1).

A. IMAGE PROCESSING

1) DATA ACQUISITION

Since agricultural spraying drones are mainly used for rice cultivation, this study obtained images of power lines in paddy fields. Pesticides are sprayed on clear or cloudy days, except on rainy days. When the sunlight and camera lens of the drone camera face each other, the image is relatively dark. Therefore, images of power lines around the paddy fields were obtained on clear or cloudy days and under various directional conditions of sunlight and camera lenses. Images were acquired using a drone equipped with a 20 million-pixel camera (DJI Phantom 4 Pro 2) at an altitude of 14–16 m for the power lines. The distance between the drone and the power line was 5–8 m.

2) LABELING

Because the power lines are in the form of thin and continuous objects, it is difficult to label them as objects such as people, animals, or cars. Some power lines are stretched in a straight line, as shown in Fig.2a, whereas others are stretched in a U-shaped curve, as shown in Fig.2b. There may be various shapes of power lines. If only the shape of the power line shown in Fig. 2a is learned, the power lines shown in Fig. 2b cannot be detected. In order to solve this problem, it is necessary to collect images of power lines of all possible shapes. It takes a lot of time. Also, if the power line is labeled with one bounding box and learned, many parts other than the power line are detected. When labeling one power line, there are cases where another power line is included as shown in Fig. 2b.

To solve this problem, the power lines are labeled with several continuous boxes of a specific size, as shown in Fig. 3. The labeling method in this study is similar to the case of lane detection using a sliding window method [15]. The brightness values of the background images above and below the power line were labeled using the bright point compared to the power line. When the power line is labeled in the method applied in this study, the position of the power line can be estimated in more detail, and significant data for learning can be obtained from a small number of images. In general, a power line is labeled in a bounding box. However, if the spacing between the two power lines is narrower than that of the bounding box, it is difficult to label the power lines individually. Thus, these two power lines are contained within one bounding box, as shown in Fig. 3. Deep learning was performed with bounding boxes of various sizes to check the performance of the power line detection according to the size of the bounding box. The size of the bounding box was changed from 0.03 to 0.15 times the ratio of the image size. The results of the bounding box for each ratio are shown in

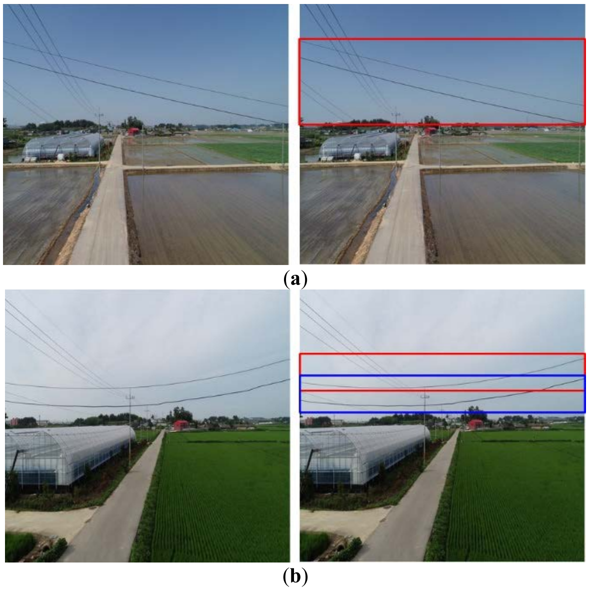

FIGURE 2. Difficulties in setting learning areas for power lines: (a) power lines from the top left to the bottom right of the image; (b) U-shaped power lines.

Fig. 4. In the case of 0.03 times bounding box, the size of the bounding box became 12 × 12 pixels because the size of the training images was 416 × 416 pixels in this study(Fig. 4a).

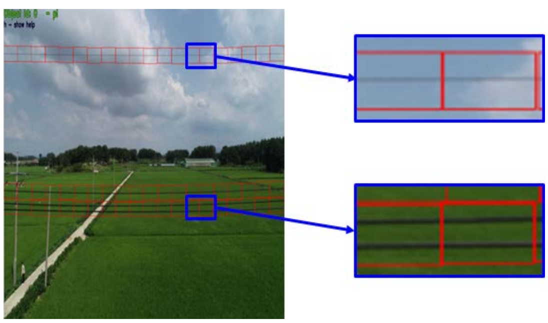

FIGURE 3. Labeling methods for single and neighboring double power lines.

B. POWER LINE DETECTION ALGORITHM

1) TINY-YOLOV3 MODEL

The tiny-YOLOv3 model is simpler than the YOLOv3 model. The detection accuracy is lower than YOLOv3, but real-time implementation is possible even with limited hardware. The tiny-YOLOv3 reduces the architecture of the darknet53. There are only seven convolution and six max-pooling layers in the basic structure, and the features are extracted using a small number of 1 × 1 and 3 × 3 convolution layers. The tiny-YOLOv3 predicts the bounding box on two different scales. One is through a feature map obtained using 13 × 13, and the other is by merging up-sampled 13 × 13 feature maps and 26 × 26 feature maps [17].

The structure of the tiny-YOLOv3 is shown in Fig. 5.

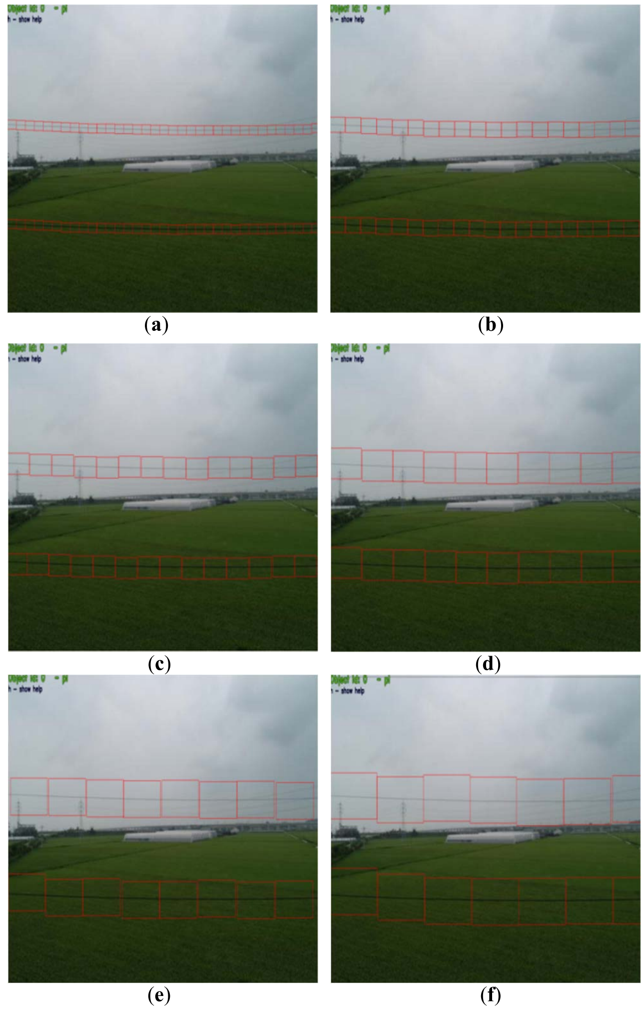

FIGURE 4. Comparison of bounding boxes for power lines according to the size ratio of the image: (a) 0.03 times; (b) 0.05 times; (c) 0.07 times; (d) 0.10 times; (e) 0.12 times; (f) 0.15 times.

2) EVALUATION METRICS

The precision and recall of the results of the deep-learning model were calculated using (1) and (2), respectively.

$$precision = TP/(TP + FP) \tag{1}$$

$$recall = TP/(TP + FN) \tag{2}$$

$$\begin{aligned} \mathrm{TP} &= \text{True Positive} \\ \mathrm{TN} &= \text{True Negative} \\ \mathrm{FP} &= \text{False Positive} \\ \mathrm{FN} &= \text{False Negative} \end{aligned}$$

The intersection over union (IoU) was used to evaluate the prediction performance of the object detector. The IoU is measured by the degree of overlap between the detected object and the ground truth using (3).

$$IoU = (Area\ of\ overlab)/(Area\ of\ union) \tag{3}$$

The average precision (AP) can be obtained as the total area of the lower part of the precision-recall graph. It is calculated

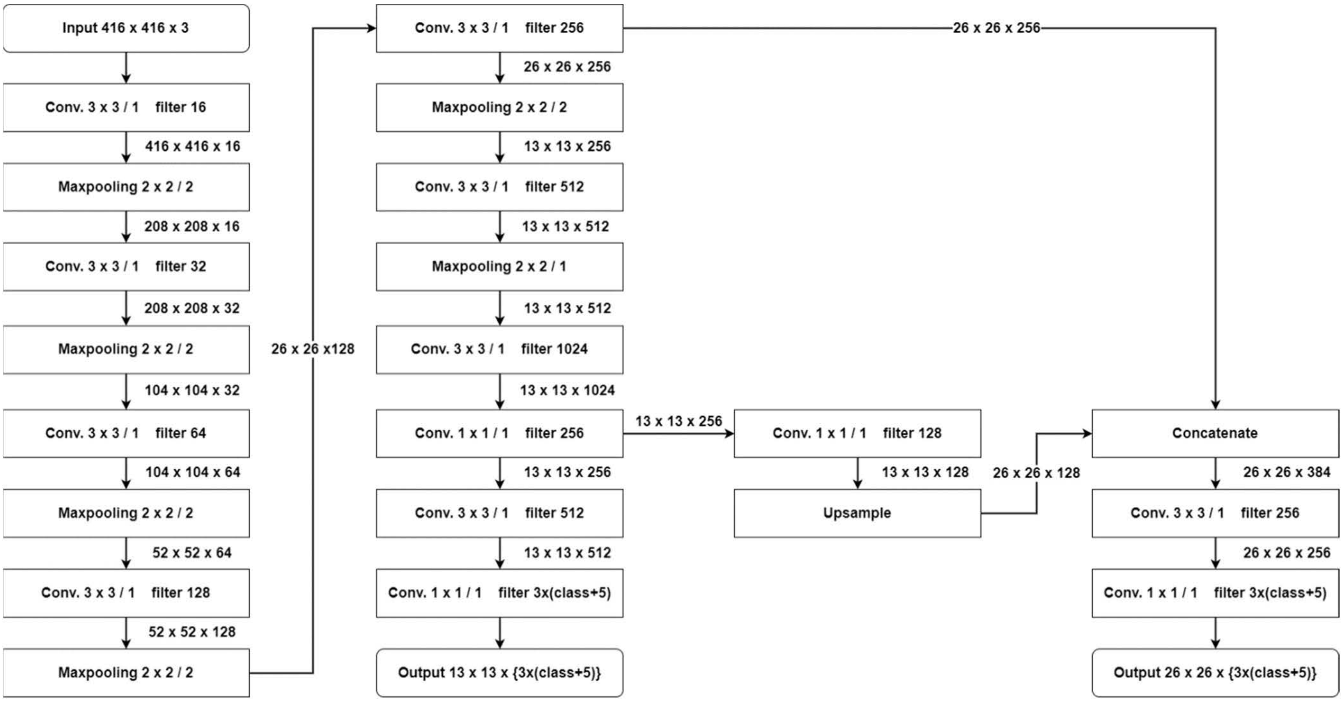

FIGURE 5. The structure of tiny-YOLOv3.

by taking the average of the maximum precision values for 11 recall values using (4) and (5) [18].

$$AP = \frac{1}{11} \sum\nolimits_{r \in \{0.0, 0.1, 0.2, \cdots, 1.0\}} P_{interp} \tag{4}$$

$$P_{interp}(\mathrm{r}) = \max_{\tilde{r}:\tilde{r} \geq r} \mathrm{p}(\tilde{r}) \tag{5}$$

where P_{interp}(r) is interpolated by taking the maximum precision measured above the recall r, and p($\tilde{r}$) is the measured precision at recall $\tilde{r}$.

PASCAL VOC is a criterion used for the category recognition and detection of visual objects. It provides standard datasets and evaluation procedures for images to the visual and machine learning communities. According to PASCAL VOC, AP is obtained when the IoU of each object is 0.5 or more. The average of the AP, mAP, evaluates whether the model is suitably trained. The mAP has been used to assess if the learning is properly performed [19]–[22].

For a single object, the ground truth was constant. However, there are several cases of ground truths for continuous objects, such as power lines. As shown in Fig. 6, both upper or lower ground truth could be possible in an image.

Fig. 7 shows a comparison between the ground truth and deep-learning results of the two cases shown in Fig. 6. Looking at the enlarged picture of the same area, the upper image of Fig. 7 shows two deep learning results (blue box) in one ground truth (green box). In the lower image of Fig. 7, one deep-learning result appears in one ground truth. The IoU value of a continuous object can be changed depending on the ground truth. The result visually seems to have all the power lines recognized, however, the mAP value was as low as 27.8 with the condition of the IoU over 0.5. Since the power lines are continuous, the IoU changes depending on how the ground truth is made. The mAP also changes according to the IoU.

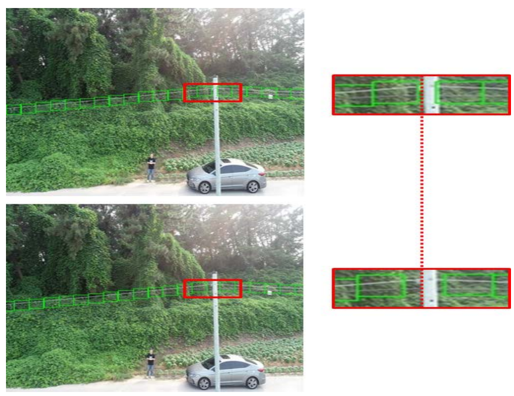

FIGURE 6. Different ground truths in the same image: the ground truth used in this paper (upper) and different ground truth (lower).

Fig. 7 shows that the power lines seem to be detected with high AP. However, if the precision and recall are calculated according to the conventional method, the AP is low. This is due to the duplicate detection of one power line. Therefore, many cases where true positives were treated as false positives would have also been included. Conversely, if all the deep-learning results from the duplicate detection are recognized as true positives, the value of recall exceeds 1 and the AP also exceeds 1. In this study, Multiple IoUs occurred in one ground truth. When the sum of IoU is 0.5 or more, it is

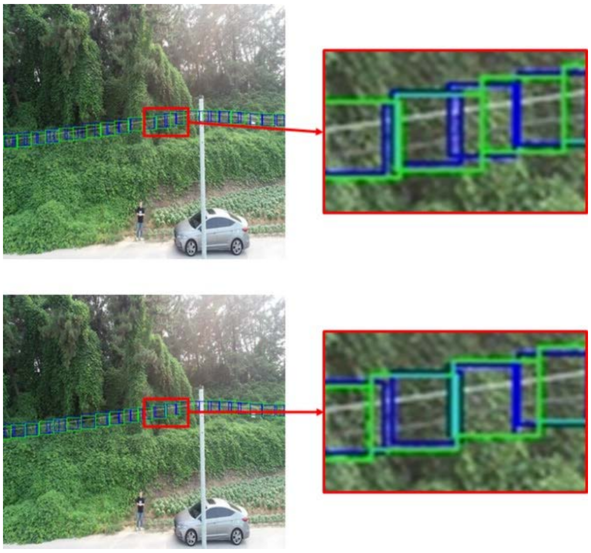

FIGURE 7. Ground truths used in this paper and the result of deep learning (upper), and different ground truth and the result of deep learning (lower) (green square: ground truth, blue square: a result of deep learning).

classified as a true positive. For example, in Fig. 8a, the first IoU is 0.25 and the second IoU is 0.15. Because the sum of IoUs becomes 0.4, it is classified as a false positive. On the other hand, as shown in Fig. 8b, if the first IoU is 0.4 and the second IoU is 0.25, the sum of IoUs is 0.65. Therefore, this case is classified as a true positive.

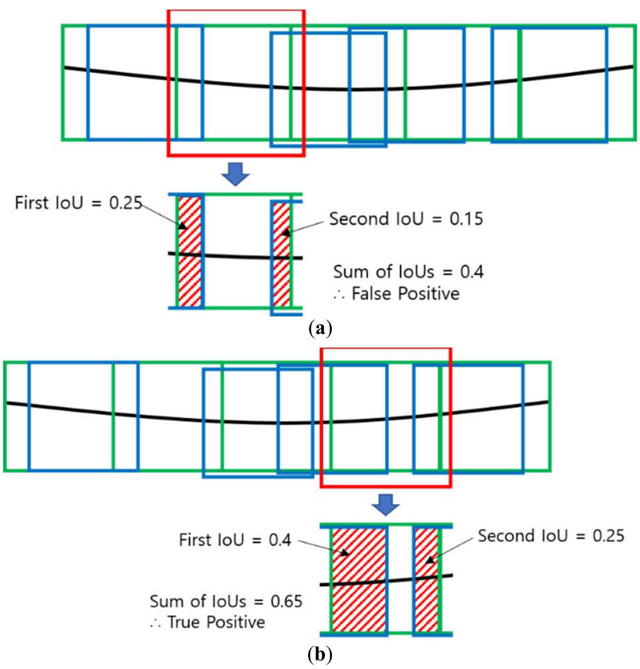

FIGURE 8. Proposed evaluation metrics: ground truth(green box), deep-learning result(blue box): (a) Example of false positives; (b) Example of true positives.

C. EMBEDDED SYSTEM AND TEST DRONE

The test drone is shown in Fig.9. It had a weight of 6.15 kg, including the battery, a payload of 5 kg, and a size of 950 × 950 × 410 mm in width × length × height. To reduce the size, weight, and power consumption of the embedded systems, the Jetson Nano (NVIDIA, USA) was chosen.

While the test drone flew, the embedded systems recorded the video of the detection results of the power lines. After the flight was completed, the performance of the deep-learning model developed in this study was validated through a video. The specifications of the embedded systems and cameras for deep-learning processing are listed in Table 1. The embedded systems were attached to the drones (Fig. 10). Indoor and field tests were conducted to validate the decided deep learning model using the test drone.

FIGURE 9. Test drone for the field tests for power line detection through deep learning.

TABLE 1. The specification of the embedded systems and camera for deep-learning processing.

	Specification
Size	100 × 80 × 29 mm (width × length × depth)
Weight	140 g
Payload	5 kg
CPU	Quad-core ARM Cortex-A57 MPCore processor
GPU	NVIDIA Maxwell architecture with 128 NVIDIA CUDA® cores
RAM	4GB 64-bit LPDDR4
OS	Ubuntu 18.04 LTS
Program	Python
GPU accelerated library	CUDA 10.0 and CUDNN 7.5
Camera	1920×1080 pixels at 30 fps

IV. EXPERIMENTAL RESULTS

A. DECISION OF DEEP LEARNING MODEL

The parameters for training the tiny-YOLOv3 are listed in Table 2. As in previous studies[23-25], the default values provided in [14] were used. The specifications of the

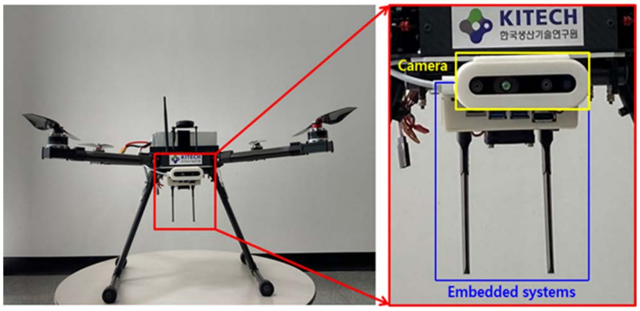

FIGURE 10. The test drone equipped with the embedded systems and camera for deep-learning processing.

deep-learning computer used in the experiment are listed in Table 3.

TABLE 2. Parameters for training power lines.

Parameter	Value
Momentum	0.9
Learning rate	0.001
Decay	0.0005
Image size	416 x 416 (pixel)
Iteration	500200

TABLE 3. The specification of the deep-learning computer.

Specification	
CPU	Intel Core i7-7700K 4.20GHz
GPU	NVIDIA GTX 1080 Ti
RAM	32GB
OS	Ubuntu 18.04 LTS
Program	Python
GPU accelerated library	CUDA 10.1 and CUDNN 7.6.5

The image data set consisted of training and test sets. The images used for training and testing were 399 and 35, respectively. Because an image includes one or more power lines, the training set contained 1146 power lines, and the test set contained 78. The power line labeling numbers for the training sets were 40231, 22315, 15376, 9801, 7404, and 6573 for each bounding box size, whereas those for the test set were 2981, 1607, 1096, 774, 602, and 417. The results are summarized in Table 4.

Fig. 11 shows the mAP values of the 35 test images, some of which are presented in Fig. 12. As the bounding box size increases from 0.05 to 0.15 times, the mAP decreases from 94.00 to 53.40. As the size of the bounding box increases, the performance of the power line detection decreases because the bounding box contains not only power lines but also objects such as trees and power poles. However, when the size

TABLE 4. Number of labeling of the training and test set according to the size of the bounding boxes.

		Training set	Test set
Number of images		399	35
Number of power lines		1146	78
Number of labeling based on the size of bounding boxes	×0.03	40231	2981
	×0.05	22315	1607
	×0.07	15376	1096
	×0.10	9801	774
	×0.12	7404	602
	×0.15	6573	417

of the bounding box is 0.03 times the image size, the mAP is 70.22, which is smaller than that of 0.05 times the image size. When the size of the bounding box becomes too small, only the black part of the power line is highlighted; thus, power line detection cannot be performed properly.

Because the highest mAP was found for the bounding box of 0.05 times the image size, the model trained on the power lines with this bounding box size was applied to the embedded systems.

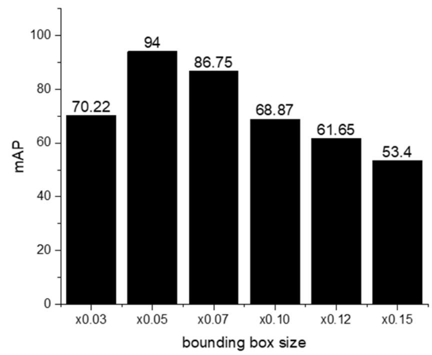

FIGURE 11. mAP of power line detection through deep learning according to the bounding box size.

In the previous study, the accuracy of power line detection was 85∼99%, and the method proposed in this paper showed that the accuracy of power line detection was 94%. In the previous study, the processing time was between 0.1 seconds and 5.55 seconds using PC. This paper obtained a processing time of 0.15 seconds using an embedded computer. This shows an above-average result than previous studies. (Table 5)

B. APPLICATION FOR THE DRONE WITH EMBEDDED SYSTEM

The decided deep-learning model was deployed on the embedded systems for the test drone. As a first validation test, an indoor experiment detected power lines 3.0 m away

FIGURE 12. Examples of test images to verify deep learning performance.

from the drone(Fig.13a). The thickness of the power lines used in the experiment was 10 mm in diameter. A power line was detected, as shown in Fig.13b. When detecting the power

TABLE 5. Performance and detection technique comparison with related works.

Ref.	Accuracy	Processing time	Detection technique	System
[4]	88%	2 s	Joint linear-time line segment detector	PC
[5]	98%	0.1 s	Hough Transform + SVM	PC
[6]	85.71%	5.55 s	Hough Transform + line tracking algorithm	PC
[8]	99.7%	0.22 s	Deep learning (CNN)	PC with GPU
[9]	85.43%	0.6 s	Deep learning (CableNet)	PC with GPU
Proposed	94%	0.15 s	Deep learning (Tiny-YOLOv3)	Embedded computer

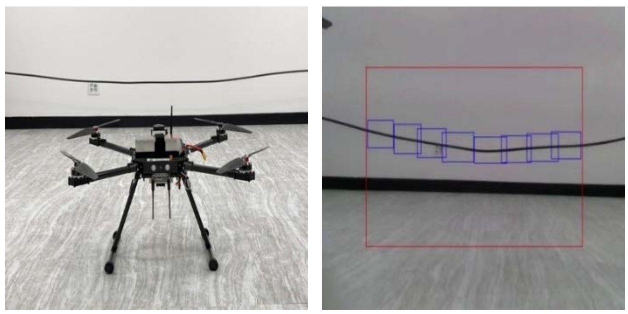

(a) (b)

FIGURE 13. Indoor experiment to validate the performance of embedded systems: (a) test drone; (b) results of power line detection.

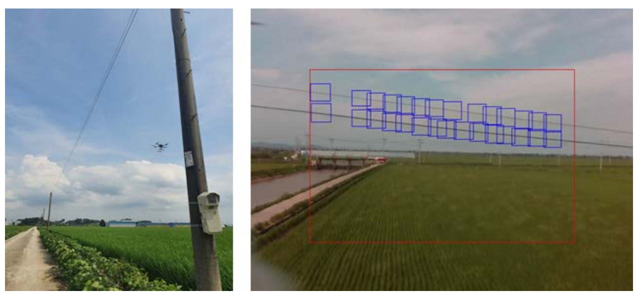

(a) (b)

FIGURE 14. Field test using the drone equipped with the embedded systems for deep-learning processing: (a) drone flying in front of power lines; (b) results of the power lines detection in real-time.

line in real-time, the FPS was evaluated to be an average of 12.5. The red border area was set as an area of collision risk, and power lines were detected in the area. Using the area of collision risk reduces the number of calculations. The field experiment was conducted using a drone equipped with embedded systems on a paddy field in Gimje-si, Jeollabuk-do. The drone flew within a 5 – 10 m distance from the power lines, and the power lines were recognized, as shown in Fig.14.

V. CONCLUSION

This paper proposes a deep-learning technique to detect the location of power lines. Because the power lines are continuous objects, the conventional object detection technique for a single object such as animals and cars is not suitable. The training set was constructed by labeling the power lines with bounding boxes of six sizes, 0.03 to 0.15 times the image size. This study proposed and applied a modified method to calculate the mAP for continuous object detection. The mAPs were evaluated to be from 53.4 to 94, and the highest mAP was found at a bounding box of 0.05 times the image size. This mAP is similar to previous studies on object detection [17], [21], [25]. This result could be concluded that if the bounding box is large, features other than the power line increase, and if the bounding box is too small, there are few features to detect the power line. The FPS 12.5 evaluated in this study is also similar to previous studies [26]–[28]. The power line detection model is installed in a lightweight embedded system with low power consumption. The drone can detect the power line during a flight in real-time. It is expected to be commercialized economically by applying it to agricultural spray drones. The limitation of this technology is that when the rice is not grown enough, the proposed algorithm can incorrectly detect ridges as power lines. Future work should include the development of a post-processing technique that detects multiple power lines and does not detect ridges as power lines. Also, an algorithm will be developed to determine the location and distance of power lines. The inference speed of the deep learning system will be improved by optimizing the deep learning model through TensorRT. This will allow agricultural spraying drones to recognize power lines and perform stop, warning, and collision avoidance.

REFERENCES

[1] S. Berrahal, J.-H. Kim, S. Rekhis, N. Boudriga, D. Wilkins, and J. Acevedo, "Border surveillance monitoring using quadcopter UAV-aided wireless sensor networks," *J. Commun. Softw. Syst.*, vol. 12, no. 1, pp. 67–82, Mar. 2016.

[2] C. Ju and H. Son, "Multiple UAV systems for agricultural applications: Control, implementation, and evaluation," *Electronics*, vol. 7, no. 9, p. 162, Aug. 2018.

[3] J. K. Park and K. Y. Jung, "Investigation and analysis of forest geospatial information using drone," *J. Korea Academia-Ind. Cooperation Soc.*, vol. 19, no. 2, pp. 602–607, 2018.

[4] X. Luo, J. Zhang, X. Cao, X. Li, and P. Yan, "Object-aware power line detection using color and near-infrared images," *IEEE Trans. Aerosp. Electron. Syst.*, vol. 50, no. 2, pp. 1374–1389, Apr. 2014.

[5] Q. Ma, D. S. Goshi, Y. C. Shih, and M. T. Sun, "An algorithm for power line detection and warning based on a millimeter-wave radar video," *IEEE Trans. Image Process.*, vol. 20, no. 12, pp. 3534–3543, Dec. 2011.

[6] L. Baker, S. Mills, T. Langlotz, and C. Rathbone, "Power line detection using Hough transform and line tracing techniques," in *Proc. Int. Conf. Image Vis. Comput. New Zealand (IVCNZ)*, Nov. 2016, pp. 1–6.

[7] F. Azevedo, A. Dias, J. Almeida, A. Oliveira, A. Ferreira, T. Santos, A. Martins, and E. Silva, "LiDAR-based real-time detection and modeling of power lines for unmanned aerial vehicles," *Sensors*, vol. 19, no. 8, p. 1812, Apr. 2019.

[8] O. E. Yetgin, B. Benligiray, and O. N. Gerek, "Power line recognition from aerial images with deep learning," *IEEE Trans. Aerosp. Electron. Syst.*, vol. 55, no. 5, pp. 2241–2252, Oct. 2019.

[9] B. Li, C. Chen, S. Dong, and J. Qiao, "Transmission line detection in aerial images: An instance segmentation approach based on multitask neural networks," *Signal Process., Image Commun.*, vol. 96, Aug. 2021, Art. no. 116278.

[10] Y. Tian, G. Yang, Z. Wang, H. Wang, E. Li, and Z. Liang, "Apple detection during different growth stages in orchards using the improved YOLO-V3 model," *Comput. Electron. Agricult.*, vol. 157, pp. 417–426, Feb. 2019.

[11] H. Zhao, Y. Zhou, L. Zhang, Y. Peng, X. Hu, H. Peng, and X. Cai, "Mixed YOLOv3-LITE: A lightweight real-time object detection method," *Sensors*, vol. 20, no. 7, p. 1861, Mar. 2020.

[12] W. F. Hendria, Q. T. Phan, F. Adzaka, and C. Jeong, "Combining transformer and CNN for object detection in UAV imagery," *ICT Exp.*, to be published, doi: 10.1016/j.icte.2021.12.006.

[13] J. Redmon and A. Farhadi, "YOLOv3: An incremental improvement," 2018, *arXiv:1804.02767*.

[14] J. Redmon. *DarkNet: Open Source Neural Networks in C—Joseph Redmon*. Accessed: Jan. 13, 2022. [Online]. Available: https://pjreddie.com/darknet

[15] K. Dinakaran, A. S. Sagayaraj, S. K. Kabilesh, T. Mani, A. Anandkumar, and G. Chandrasekaran, "Advanced lane detection technique for structural highway based on computer vision algorithm," *Mater. Today, Proc.*, vol. 45, pp. 2073–2081, 2021.

[16] M. Basso and E. Pignaton de Freitas, "A UAV guidance system using crop row detection and line follower algorithms," *J. Intell. Robotic Syst.*, vol. 97, nos. 3–4, pp. 605–621, Mar. 2020.

[17] W. Gai, Y. Liu, J. Zhang, and G. Jing, "An improved tiny YOLOv3 for real-time object detection," *Syst. Sci. Control Eng.*, vol. 9, no. 1, pp. 314–321, Jan. 2021.

[18] M. Everingham, L. Van Gool, C. K. I. Williams, J. Winn, and A. Zisserman, "The Pascal visual object classes (VOC) challenge," *Int. J. Comput. Vis.*, vol. 88, no. 2, pp. 303–338, Sep. 2009.

[19] Y. Nie, P. Sommella, M. O'Nils, C. Liguori, and J. Lundgren, "Automatic detection of melanoma with Yolo deep convolutional neural networks," in *Proc. E-Health Bioeng. Conf. (EHB)*, Nov. 2019, pp. 1–4.

[20] Q.-C. Mao, H.-M. Sun, Y. B. Liu, and R.-S. Jia, "Mini-YOLOv3: Real-time object detector for embedded applications," *IEEE Access*, vol. 7, pp. 133529–133538, 2019.

[21] D. Wang, W. Li, X. Liu, N. Li, and C. Zhang, "UAV environmental perception and autonomous obstacle avoidance: A deep learning and depth camera combined solution," *Comput. Electron. Agricult.*, vol. 175, Aug. 2020, Art. no. 105523.

[22] H. C. Bazame, J. P. Molin, D. Althoff, and M. Martello, "Detection, classification, and mapping of coffee fruits during harvest with computer vision," *Comput. Electron. Agricult.*, vol. 183, Apr. 2021, Art. no. 106066.

[23] E. Lygouras, N. Santavas, A. Taitzoglou, K. Tarchanidis, A. Mitropoulos, and A. Gasteratos, "Unsupervised human detection with an embedded vision system on a fully autonomous UAV for search and rescue operations," *Sensors*, vol. 19, no. 16, p. 3542, Aug. 2019.

[24] M. Elgendy, C. Sik-Lanyi, and A. Kelemen, "A novel marker detection system for people with visual impairment using the improved tiny-YOLOv3 model," *Comput. Methods Programs Biomed.*, vol. 205, Jun. 2021, Art. no. 106112.

[25] J. Gong, J. Zhao, F. Li, and H. Zhang, "Vehicle detection in thermal images with an improved yolov3-tiny," in *Proc. IEEE Int. Conf. Power, Intell. Comput. Syst. (ICPICS)*, Jul. 2020, pp. 253–256.

[26] M. J. Shafiee, B. Chywl, F. Li, and A. Wong, "Fast YOLO: A fast you only look once system for real-time embedded object detection in video," 2017, *arXiv:1709.05943*.

[27] M. Ikhlayel, A. J. Iswara, A. Kurniawan, A. Zaini, and E. M. Yuniarno, "Traffic sign detection for navigation of autonomous car prototype using convolutional neural network," in *Proc. Int. Conf. Comput. Eng., Netw., Intell. Multimedia (CENIM)*, Nov. 2020, pp. 205–210.

[28] N. Ayoub and P. Schneider-Kamp, "Real-time on-board deep learning fault detection for autonomous UAV inspections," *Electronics*, vol. 10, no. 9, p. 1091, May 2021.

HYUN-SIK SON was born in Ulsan, Republic of Korea, in 1989. He received the B.S. and M.S. degrees from the Department of Electrical and Electronic Engineering, Pusan National University, in 2015 and 2017, respectively. He is currently pursuing the Ph.D. degree with the Department of Electrical and Computer Engineering, Pusan National University.

Since 2017, he has been working as a Research Assistant with the Smart Agricultural Machinery Research and Development Group, Korea Institute of Industrial Technology. His research interests include artificial intelligence, autonomous driving, and deep learning.

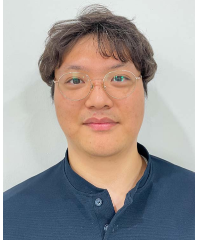

DEOK-KEUN KIM received the B.S. and M.S. degrees in biosystem engineering from Chonnam National University, Gwangju, South Korea, in 2016 and 2019, respectively, where he is currently pursuing the Ph.D. degree with the Interdisciplinary Program in Agricultural and Life Science.

Since 2005, he has been working as a Research Assistant with the Smart Agricultural Machinery Research and Development Group, Korea Institute of Industrial Technology. His research interests include the development of the smart farm, agricultural robots, and precision agriculture.

SEUNG-HWAN YANG was born in Seoul, Republic of Korea, in 1979. He received the B.S. degree in agricultural machinery engineering and the M.S. and Ph.D. degrees in biosystems engineering from Seoul National University, in 2002, 2007, and 2011, respectively.

From 2002 to 2005, he was a Computer Programmer with IBK System and the Syswill. From 2011 to 2013, he was a Postdoctoral Researcher with the Korea Research Institute of Standards and Science. Since 2013, he has been a Principal Researcher with the Smart Agricultural Machinery Research and Development Group, Korea Institute of Industrial Technology. He has participated in more than 40 research projects. He is the author of more than ten articles and more than ten patents. His research interests include agricultural automation and robotics using the IoT, ICT, and AI technology.

YOUNG-KIU CHOI received the B.S. degree in electrical engineering from Seoul National University, Seoul, South Korea, in 1980, and the M.S. and Ph.D. degrees in electrical engineering from the Korea Advanced Institute of Science and Technology (KAIST), Seoul, in 1982 and 1987, respectively.

He was a Visiting Scholar at the California Institute of Technology, Pasadena, CA, USA, from 1990 to 1991, and a Visiting Professor at the University of Southwestern Louisiana, Lafayette, IN, USA, from 1998 to 1999. Since 1986, he has been a Professor with the Department of Electrical and Computer Engineering, Pusan National University, Pusan, South Korea. His research interests include intelligent control, evolutionary algorithms, variable-structure control, robotics, and power electronics.